Internal ionization of Ar and Kr noble-gas cryocrystals by the excitation energy of trapped metastable excited atoms

1995 J. Phys.: Condens. Matter 7 2819

(http://iopscience.iop.org/0953-8984/7/14/019)

J. Phys.: Condens. Matter 7 (1995) 2819–2828. Printed in the UK

Internal ionization of Ar and Kr noble-gas cryocrystals by the excitation energy of trapped metastable excited atoms

R A Zhitnikov and Yu A Dmitriev

A F Ioffe Physico-Technical Institute, 26 Politechnicheskaya Street, St Petersburg 194021, Russia

Received 18 July 1994, in final form 7 December 1994

Abstract. Local metastable excited states are found in Ar and Kr cryocrystals when He gas-discharge products are trapped in the growing cryocrystals. These states are detected by ESR and are interpreted as being local metastable excited $np^5(n+1)s\,^3P_2$ atomic-type states in Ar and Kr cryocrystals. The study showed that the yield of the $^3P_2$ excitations in the above process decreases with increasing temperature. Analysis of the results allows the following explanation of the observed effect to be given. Metastable excited He atoms from the He gas discharge are trapped in the growing Ar or Kr cryocrystals and transfer their excitation energy to the cryocrystal to form, in the process of internal ionization, a RG^+ ion and a free electron in the conduction band, whereupon the fast (10^{-12} s) self-trapping reaction of a hole follows: $RG^+ + RG \rightarrow RG_2^+$. Thereafter either the dissociative recombination reaction $RG_2^+ + e \rightarrow RG_2^{**} \rightarrow RG + RG^*(^3P_2)$ or recombination $RG_2^+ + e \rightarrow RG + RG$ to produce ground-state atoms could take place. The former is likely at lower temperatures, and the latter at higher temperatures when the vibrational relaxation rate of the RG^+ molecular ion increases and the mobility of free electrons in the conduction band decreases. This is the reason for the observed temperature dependence.

1. Introduction

In this paper, we report the detection and investigation of a new phenomenon: internal ionization of the noble-gas cryocrystals Ar and Kr by He gas-discharge excited products (metastable $2\,^3S_1$ and $2\,^1S_0$ He atoms) trapped in the growing cryocrystals followed by the formation in these cryocrystals of local metastable excited $^3P_2$ atomic-type states.

In the recent work by Zhitnikov and Dmitriev (1993, 1994), a new effect has been detected and studied: quasi-resonance transfer of the excitation energy from a trapped excited metastable atom to a noble-gas cryocrystal. The effect is evidenced in the transfer of the excitation energy from the metastable excited $2\,^3S_1$ He atom trapped in the growing neon cryocrystal to the exciton energy band of the neon crystal. This process is followed by the exciton self-trapping into the $2p^53p$ state and its subsequent decay to the lowest excited $2p^53s\,^3P_2$ state recorded, in our experiment, by ESR.

The local metastable excited $np^5(n+1)s\,^3P_2$ atomic-type states in Ne, Ar, Kr and Xe noble-gas cryocrystals were previously obtained (Zhitnikov *et al* 1991, 1992) by the direct trapping in the growing cryocrystal of free excited metastable $^3P_2$ noble-gas atoms which form in the discharge in a noble gas of the same kind; the excited $^3P_2$ atomic-type states in the cryocrystals are detected by ESR.

It has also been noted by Zhitnikov and Dmitriev (1994) that weak signals related to the Ar and Kr excited $np^5(n+1)s\,^3P_2$ atomic-type states were recorded in these cryocrystals as products of the strong continuous He discharge were trapped in the growing cryocrystals,

0953-8984/95/142819+10$19.50

Ar or Kr gas, respectively, being passed to the substrate, avoiding the gas-discharge active part.

All energy levels of Ar and Kr atoms lie far below the lowest excited He level, and therefore the excitation energy cannot be transferred from the metastable excited He atom to the exciton bands of Ar and Kr cryocrystals through either a resonance or a quasi-resonance process.

This work is aimed at investigation and explanation of the new phenomenon discovered in Ar and Kr cryocrystals subject to the action of excited particles from a strong He gas discharge.

2. Experimental results

The experimental set-up used here has been described earlier (Zhitnikov and Dmitriev 1994). The solid samples under study were obtained by condensation of the matrix gas on the thin-walled bottom of a quartz finger filled with liquid helium; the bottom of the quartz finger was used here as the substrate and was located at the centre of the microwave cavity of the ESR spectrometer. The products of the high-frequency He gas discharge were aimed without intermediate feeding tubes directly onto the substrate, which prevented them from decay on the walls of the tubes. The set-up and technique allowed us to obtain directly, in the cavity of the ESR spectrometer, samples of noble-gas cryocrystals which trap gas-discharge products with growth. This makes it possible to detect unstable short-lived excited states which form in the cryocrystals.

Figure 1 shows the main part of the experimental set-up. Here 1 is the cylindrical microwave cavity of the X-band ESR spectrometer, 2 is the bottom of the quartz finger 3, filled with liquid helium, and 4 is a waveguide. The bottom 2 of the quartz finger is a low-temperature substrate for the gases being condensed. An electrodeless high-frequency gas discharge is excited in the glass tube 5 with an outlet 6 of 0.2 mm diameter. The matrix gas could be supplied to the substrate 2 by a glass tube 7 and further by a quartz tube 8 inserted into the cavity. The end of the quartz tube 8 is located close (3 mm) to the bottom 2 of the quartz finger, which facilitates effective freezing of the matrix gas.

The whole device presented in figure 1 is cooled externally with liquid-nitrogen (LN_2) vapour and the temperature of the device can be varied from 77 to 300 K.

A high-frequency (14 MHz) oscillator is used to maintain the discharge. The high-frequency power is fed through a coaxial cable to the coil 9 wound over the gas discharge tube 5.

The experimental procedure is as follows. Pure He gas was passed through the liquid-nitrogen-vapour-cooled gas discharge tube 5, in which an electrodeless high-frequency discharge was excited. Ground-state He atoms together with gas-discharge products passed through the outlet 6 of the discharge tube 5 into the evacuated cavity and reached the bottom 2 of the quartz finger 3 filled with liquid helium at 2.2–4.2 K. Pure Ar or Kr gas, also cooled by liquid-nitrogen vapour, was passed through the tubes 7 and 8, avoiding the gas discharge, onto the substrate. The Ar or Kr gas flow rate to the substrate is an order of magnitude greater than the He gas flow rate to the substrate. The ESR spectra of the sample were recorded continuously during its condensation, i.e. growth of the argon or krypton crystal with He gas-discharge products trapped in the sample. The short-lived centres were separated from the stable centres by switching off the discharge, i.e. switching off the voltage on the coil 9 during the recording of the ESR spectrum.

Figure 2 shows the ESR spectra of the growing argon and krypton cryocrystals which trap He gas-discharge products. All lines in the figure have g-factors of 1.99986(12) and

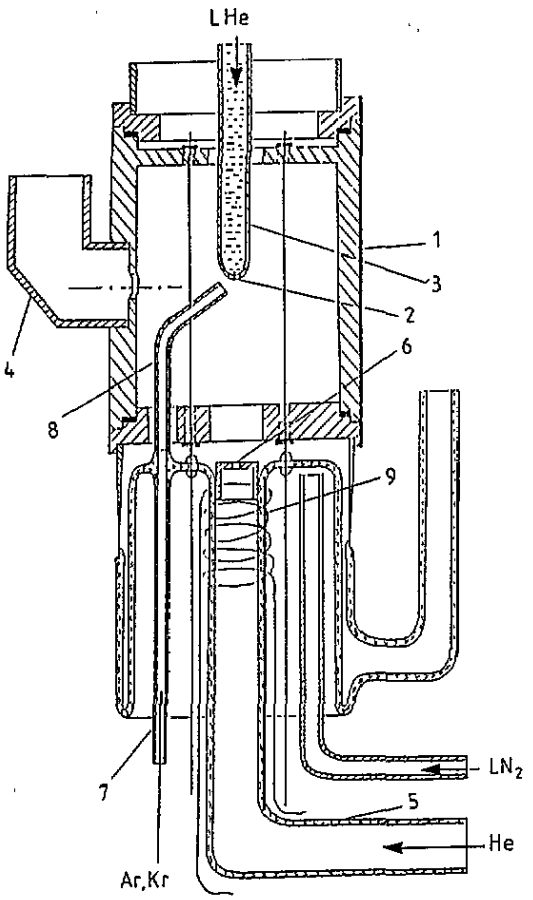

Figure 1. The main part of the experimental set-up (for notation, see the text).

linewidths of 0.1–0.2 G. The small linewidth and symmetric lineshape suggest that the lines correspond to isotropic centres, whereas the sample is presumably polycrystalline. These spectra were observed only during the Ar or Kr gas condensation and disappeared at the instant when the He discharge was turned off. On the other hand, no ESR spectra were observed in experiments where He flow was passed through the tube 5 with the discharge on but with no Ar or Kr gas being fed onto the substrate through the inlet tubes. We found that the He gas discharge used cannot provide any ESR spectra before the Ar (Kr) condensation nor after the Ar (Kr) flow has been turned off despite a solid Ar (Kr) layer condensed on the substrate 2 in a long time run.

The fact that the lines of the spectra recorded here are identical in all their characteristics with those of the pure Ar and Kr spectra (Zhitnikov *et al* 1991, 1992) means that the present spectra and the pure-gas spectra are due to centres of the same type and permits us to give an explanation of the nature of the present centres in the same way as has been done previously (Zhitnikov *et al* 1991, 1992, Zhitnikov and Dmitriev 1993, 1994). Namely, the centres observed here can be interpreted as being metastable excited $np^5(n+1)s\,^3P_2$ atomic-type states which become localized in a face-centred cubic (FCC) Ar (Kr) crystal lattice, shift the nearest matrix atoms outwards, rearrange their surroundings and are subject

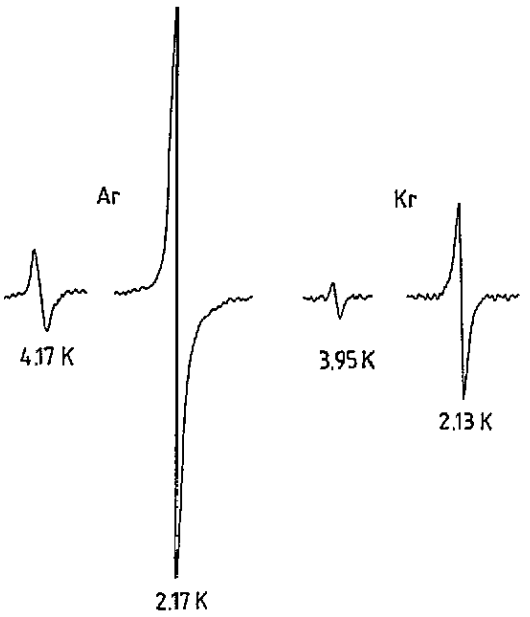

Figure 2. EPR signals of the $^3P_2$ centres recorded at two temperature points, which arise as the He gas-discharge products are trapped in a growing Ar or Kr cryocrystal. The spectrometer gains for the low- and high-temperature signals related to the corresponding cryocrystal, Ar or Kr, are the same. All observed lines have g-factors of 1.999 86(12).

to the action of the anisotropic electric field of this environment which, being rearranged, is no longer of cubic symmetry.

After the discovery in Ar and Kr cryocrystals of the ESR spectra presented in figure 2, the dependence of the production probability of the local excited $^3P_2$ atomic-type state in the cryocrystals on the sample temperature was studied. With this goal in mind, the signal intensity of the above spectra was measured as a function of the substrate temperature. The substrate temperature or, correspondingly, the temperature of the sample growing on the substrate 2 (figure 1) was lowered by pumping the boiled-off gas from the liquid-He bath. The sample temperature was measured by monitoring the helium vapour pressure over the liquid-helium surface.

Shown in figure 3 are the temperature dependences of the ESR line intensities which are typical of Ar (curve 1) and Kr (curve 2) cryocrystals. The ESR lines are like those depicted in figure 2. For reference, the temperature dependence of the ESR line intensity for the growing Ne cryocrystal which traps the metastable He atoms is also plotted. This is based on the previous findings by Zhitnikov and Dmitriev (1994). For convenient comparison, the ESR signal intensities are measured in $A(T)/A(T_0)$ units, where $T_0 = 4.22$ K for the Ne cryocrystal and, for the Ar and Kr cryocrystals, T_0 is the lowest temperature at which the sample is still sufficiently stable. Being condensed on a cold substrate, the noble-gas (Ne, Ar, Kr or Xe) solid sample absorbing the He gas was subject to spontaneous partial destruction at intervals. The destruction looked like a small 'explosion' of part of the sample and momentarily broke the device vacuum; the signal intensity appreciably decreased before the 'explosion' as well as immediately after it. After the 'explosion' had ended, the device vacuum and the ESR signal intensity were rapidly restored so that a reliable measurement of the signal intensity–temperature dependence could be taken. However, the

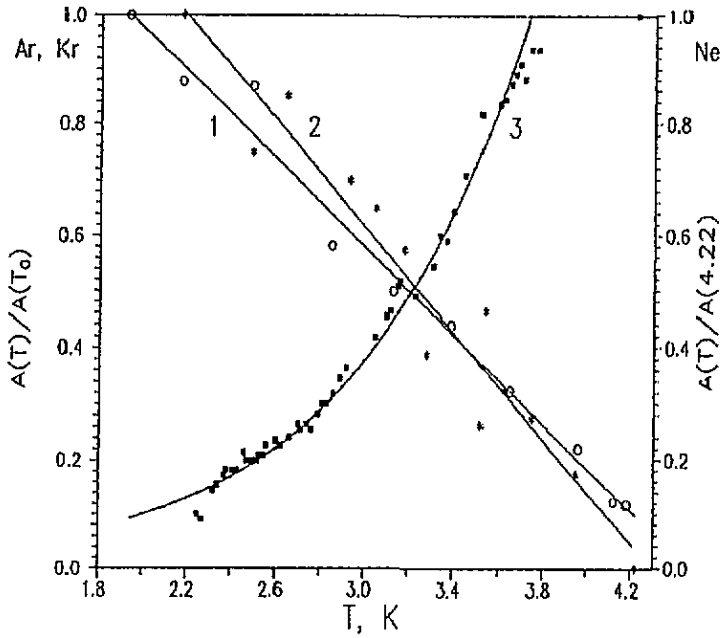

Figure 3. Temperature dependences of the ESR signal amplitude for the $^3P_2$ centres which form in growing Ar (line 1, ○) Kr (line 2, ∗) and Ne (curve 3, ■) cryocrystals as these cryocrystals trap He gas-discharge products.

'explosion' frequency increased with decreasing temperature and became sufficiently high, at temperatures close to and below 2 K, to prevent signals from re-establishing and to give no way of measuring as the temperature was lowered further. This gave the measurement of the lowest possible temperature T_0 which changed somewhat from run to run.

It is evident from figure 3 that the temperature dependence of the ESR signal intensity, i.e. the temperature dependence of the production probability of the atomic-type $^3P_2$ excitations in Ar and Kr cryocrystals, can be well fitted by a linear function $A(T)/A(T_0) = -a(T-T_0)+b$. The experiments carried out showed that the line slope, or the magnitude of a, varied within narrow limits comparable, presumably, with those of experimental error. A set of six experiments with Ar yields a(Ar) changing from 0.33 to 0.44, an average quantity being $\overline{a(\mathrm{Ar})} \simeq 0.39$, while three Kr runs give $a(\mathrm{Kr}) = 0.31$–0.57 and $\overline{a(\mathrm{Kr})} \simeq 0.46$. In these experiments, b ranges between 1.66 and 1.93 for Ar ($\overline{b(\mathrm{Ar})} = 1.78$), and between 1.82 and 2.38 for Kr ($\overline{b(\mathrm{Kr})} = 2.11$). The plots in figure 3 are not corrected for the temperature dependence of the Boltzmann population distribution over the paramagnetic centre Zeeman sublevels. It is difficult to account explicitly for the correction because the relationship between the $^3P_2$ centre lifetime τ in Ar and Kr and the spin–lattice relaxation time T_1 is still uncertain. If τ is not greater than T_1, then thermal equilibrium has no time to become established before the centre decays; so the Boltzmann correction becomes smaller. The plots in figure 3 have been estimated to depart only slightly from linear when corrected for the Boltzmann distribution at thermal equilibrium. The principal inference about the monotonic increase in $A(T)/A(T_0)$ with decreasing temperature remains intact. Previously (Zhitnikov and Dmitriev 1994), in the case of the neon cryocrystal trapping the metastable $2\,^3S_1$ He atoms, the temperature dependence has been shown to be exponential ('Arrhenius-like') $A(T)/A(T_0) = \exp[-(E/k)(1/T - 1/T_0)]$, where $E = 12(6)K = 0.0010(5)$ eV.

Thus, the temperature dependences of the $^3P_2$-centre production probability are closely related for the Ar and Kr cryocrystals while quite distinct from that of the Ne cryocrystal in both the trend and the shape. Attempts at obtaining paramagnetic centres and their ESR spectra in the growing Xe cryocrystal trapping the He gas-discharge products have not been successful. A conceivable reason for this is discussed below.

3. Interpretation

From the preceding section, it follows that the local metastable excited $np^5(n+1)s\ ^3P_2$ atomic-type states form in the growing Ar and Kr cryocrystals trapping helium gas-discharge products as they also do in the growing Ne cryocrystal trapping from the gas discharge the metastable excited $2\,^3S_1$ He atoms. However, the process of the quasi-resonance energy transfer from the metastable He atom to the cryocrystal exciton band which occurs in the case of Ne will not do so for the Ar and Kr cryocrystals. This is because all energy levels and exciton bands of the Ar and Kr cryocrystals as well as the energy levels of the corresponding free atoms lie far below the lowest excited He level. Thus the mechanism of the energy transfer from He gas-discharge products and production of metastable excited $^3P_2$ states in the Ne cryocrystal differ fundamentally from those occurring in Ar and Kr, which also follows from figure 3 showing the Ne temperature dependence of the $^3P_2$ production probability quite distinct from those of Ar and Kr.

On examination of the experimental results outlined in the preceding section, the following mechanism of formation of the metastable $^3P_2$ states in the growing Ar and Kr cryocrystals subjected to the action of He discharge products can be proposed.

Previous experiments on Ne cryocrystals (Zhitnikov and Dmitriev 1994) which are similar to the present study in the experimental procedure suggest that the noble-gas cryocrystals, as they grow, trap a quantity of the metastable excited He atoms large enough to produce a continuous abundance of local metastable excited $^3P_2$ atomic-type states, yielding intense ESR spectra. There is no question that the metastable $2\,^3S_1$ and $2\,^1S_0$ He atoms are trapped, in the present study, in great numbers in the growing Ar and Kr cryocrystals, for the trapping process occurs in these cryocrystals as it evidently does in Ne (Zhitnikov and Dmitriev 1994). The excitation energies of the metastable He atoms $E(2\,^3S_1) = 19.82$ eV and $E(2\,^1S_0) = 20.62$ eV are considerably larger than the energy gaps of the Ar and Kr cryocrystals: $E_g(\mathrm{Ar}) = 14.16$ eV and $E_g(\mathrm{Kr}) = 11.61$ eV (Schwentner *et al* 1985, p 27). Therefore, the trapped metastable $2\,^3S_1$ and $2\,^1S_0$ He atoms must transfer their excitation energies to the Ar or Kr cryocrystal to produce internal ionization of this cryocrystal when a hole, i.e. Ar^+ or Kr^+ ion, arises in the valence band while a free electron e appears in the conduction band. It is known (Belov *et al* 1981) that, in the noble-gas cryocrystals, holes become self-trapped in a very short time (10^{-12}–10^{-13} s) after their production to give rise to molecular ions: $\mathrm{RG}^+ + \mathrm{RG} \rightarrow \mathrm{RG}_2^+$. Occupying first a vibrationally excited level, the molecular ion relaxes to the lowest vibrational levels, transferring its energy to the phonon spectrum of the cryocrystal. At some time a free electron in the conduction band encounters a hole to recombine with it and to produce an excited RG_2^{**} molecule which may, on occasion, dissociate, yielding an excited atom: $\mathrm{RG}_2^+ + \mathrm{e} \rightarrow \mathrm{RG}_2^{**} \rightarrow \mathrm{RG}^* + \mathrm{RG}$. The process is known to occur both in the noble gases and in their cryocrystals (Belov *et al* 1981). This reaction of dissociative recombination may be one way to produce ultimately the metastable excited $^3P_2$ atomic-type states in Ar and Kr cryocrystals observed in the present study.

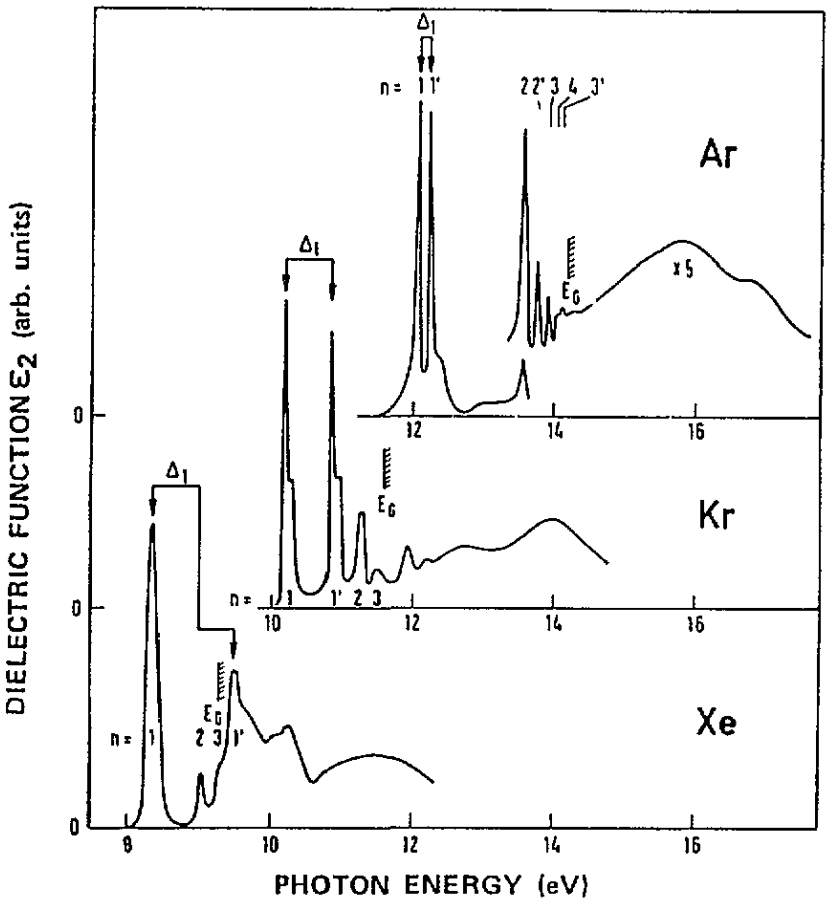

Figure 4. Optical absorption spectra of the Ar, Kr and Xe cryocrystals.

Next we discuss in greater detail the plausible mechanisms of production, in Ar and Kr cryocrystals, of the excited $np^5(n+1)s\,^3P_2$ states that we have recorded.

Figure 4 gives the optical absorption spectra of the Ar, Kr and Xe cryocrystals (Schwentner *et al* 1985, figure 3.9). Figure 5 presents the schematic diagrams of the energy levels, zones and exciton bands of the Ar and Kr cryocrystals. Also shown are the feasible molecular- and atomic-type excited states of these cryocrystals. The schematic diagram in figure 5(*a*) for the Ar cryocrystal is taken from the paper by Belov *et al* (1981) whereas figure 5(*b*) for the Kr cryocrystal, which we ourselves have drawn, is based on figure 4 and the monograph by Schwentner *et al* (1981, figures 3.10, 3.11 and table 3.4).

The process of formation of the $3p^54s\,^3P_2$ states (figure 5(*a*)) in Ar cryocrystals having trapped the metastable $2\,^3S_1$ and $2\,^1S_0$ He atoms from the helium gas discharge can be conceived as follows.

The trapped $2\,^3S_1$ and $2\,^1S_0$ He atoms transfer their excitation energies to the Ar cryocrystal, with the consequent above-mentioned internal ionization of the cryocrystal which results in the formation of a free electron in the conduction band and a hole Ar^+ in the valence band; the hole becomes rapidly (in a time of 10^{-12}–10^{-13} s) self-trapped, i.e. turns into the vibrationally excited molecular Ar_2^+ ion. The energy levels of the Ar_2^+ ion

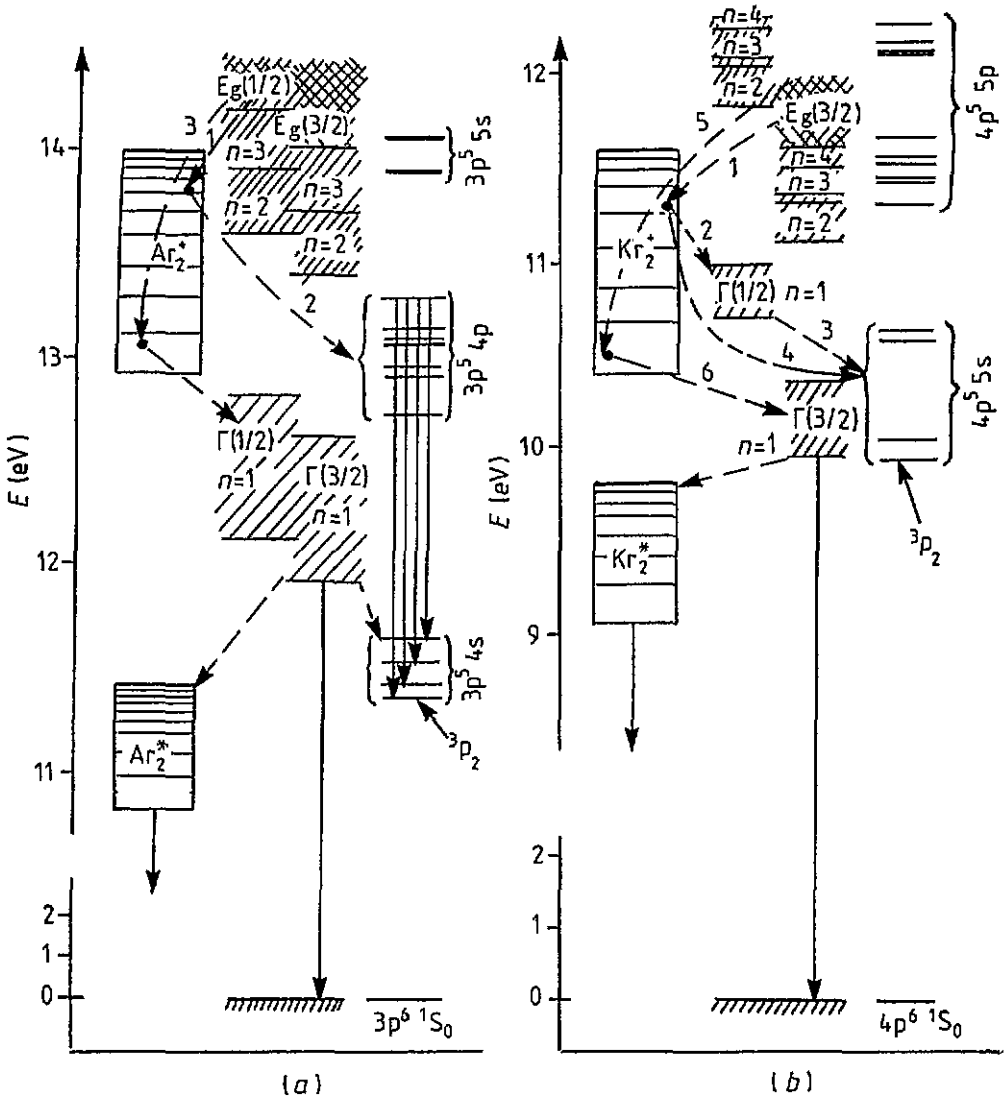

Figure 5. Schematic diagrams of the energy levels and bands for the excited states of the Ar and Kr cryocrystals.

are shown in figure 5(*a*). Provided that, after a short time, a free electron moving in the conduction band encounters and recombines with an Ar_2^+ hole which has had no time to relax vibrationally, through path 1 in figure 5(*a*), the reaction of dissociative recombination shown in figure 5(*a*) (path 2) is possible: $Ar_2^+ + e \rightarrow Ar_2^{**} \rightarrow Ar + Ar^*(3p^5 4p)$. The reaction is followed by the decay of the excited atom $Ar^*(3p^5 4p) \rightarrow Ar^*(3p^5 4s)$ to form the $(3p^5 4s)$ $^3P_2$ state that we have observed by ESR. This is likely to be the mechanism of formation, in Ar cryocrystals, of the metastable excited $^3P_2$ atomic-type states as the excitation energy is being transferred from the metastable He atoms to the cryocrystal.

Suppose that the time that a free electron moving in the conduction band takes to approach an Ar_2^+ molecular ion is sufficiently long that the ion has relaxed to the lowest

vibrational state (path 3 in figure 5(*a*)). Then, as is seen from figure 5(*a*), the energy released during the $Ar_2^+ + e$ recombination is allowed to transfer to the exciton band with $n = 1$ (path 4 in figure 5(*a*)). This exciton then can either decay to the ground state or become self-trapped to the two-centre excimer state Ar_2^*, which also decays to two ground-state Ar atoms. These processes cannot lead to the formation of the atomic-type $^3P_2$ state. That is why the process of production of the atomic-type $^3P_2$ state through the recombination of the vibrationally relaxed Ar_2^+ molecular ion, while not eliminated (e.g. by the self-trapping of the exciton with $n = 1$ to the $3p^5 4s$ atomic-type states), should be far less probable than the dissociative recombination of the vibrationally excited Ar_2^+ ion (path 2 in figure 5(*a*)). Which of the two processes, paths 1 and 2 or paths 3 and 4 in figure 5(*a*), occurs in a particular experiment depends on the cryocrystal growth temperature. With increasing sample temperature the vibrational relaxation rate of the Ar_2^+ molecular ion rises, whereas the mobility of electrons in the conduction band decreases, leading to an increase in the time separation between the Ar_2^+ ion production and its recombination with an electron with increasing sample temperature. All these factors have the effect of reducing the probability of the dissociative recombination (paths 1 and 2 in figure 5(*a*)) and consequently the yield of $^3P_2$ centres, which underlies the temperature dependence that we have found for Ar (figure 3). Correspondingly, the probability of the excitation energy transfer to the exciton band with $n = 1$ (paths 3 and 4 in figure 5(*a*)) followed by decay to two ground-state Ar atoms increases with increasing sample temperature.

In the Kr cryocrystal, the energy schematic diagram of which is shown in figure 5(*b*), processes must be somewhat different from those described above for Ar. Metastable He atoms trapped in the growing Kr cryocrystal will also cause internal ionization of the cryocrystal to produce in a short time (10^{-12}–10^{-13} s) a vibrationally excited self-trapped hole Kr_2^+ and a free electron in the conduction band. It is evident from figure 5(*b*) that at low temperatures, when a molecular ion Kr_2^+ recombining with an electron should be vibrationally excited (path 1 in figure 5(*b*)), the most likely mechanism of the energy loss is that through the excitation energy transfer to the exciton band with $n = 1$, $\Gamma(\frac{1}{2})$ (path 2) followed by self-trapping to the $4p^5 5s$ state (path 3) and production of the excited $^3P_2$ state detected in the experiment by ESR. The energy gap between the $\Gamma(\frac{1}{2})$ and $\Gamma(\frac{3}{2})$ subbands of the exciton with $n = 1$ must hamper non-radiative transitions from the first subband to the second in the process. It seems possible that the dissociative recombination $Kr_2^+ + e \rightarrow Kr_2^{**} \rightarrow Kr + Kr(4p^5 5s)$ can also contribute to the observed signal, giving the metastable $^3P_2$ state as shown in figure 5(*b*), path 4. As the sample temperature increases, the vibrational relaxation of the Kr_2^+ molecular ion speeds up while the movement of electrons in the conduction band slows down. This forces the recombination $Kr_2^+ + e$ to proceed through path 5, figure 5(*b*), in which case the excitation energy is likely to be transferred to the exciton band with $n = 1$, $\Gamma(\frac{3}{2})$ (path 6) with subsequent decay to the ground state either immediately from the subband with $n = 1$, $\Gamma(\frac{3}{2})$, or through the self-trapped excimer Kr_2^* state. This will lead to a decrease in the yield of the metastable excited $^3P_2$ states as the cryocrystal temperature increases. The processes discussed above are responsible for the decrease in the $^3P_2$ centre yield in the Kr cryocrystal with increasing temperature. It is of interest that the temperature dependences of the probability of the $^3P_2$ centre formation for Ar and Kr cryocrystals are similar in appearance (figure 3), notwithstanding certain distinctions between mechanisms of production of these metastable excited atomic-type centres.

As noted in the previous section, attempts to detect an ESR spectrum related to the centres arising in a growing Xe cryocrystal which is subject to the action of the He gas discharge have failed. The possible reason is that, as discussed by Belov *et al* (1981), the

Xe cryocrystal exciton bands overlap, forming a series of closely spaced energy levels up to the conduction band, which benefits fast excitation relaxation to the state with $n = 1$, $\Gamma(\frac{3}{2})$, and prevents formation of the local excited atomic-type states.

Not only does the growing noble-gas cryocrystal trap metastable excited $2\,^3S_1$ and $2\,^1S_0$ He atoms, the effect being evidently proved in our experiments, but also the surface of the cryocrystal is exposed to the VUV helium gas-discharge irradiation with photon energies equal to and higher than 21 eV. Penetrating into the Ar or Kr cryocrystal, the irradiation is capable of causing internal ionization just as the excited metastable $2\,^3S_1$ (19.8 eV) and $2\,^1S_0$ (20.6 eV) He atoms do with the subsequent processes and dependences, including the temperature dependence, discussed above. It is noted, however, in section 1, that, after the Ar or Kr gas flow onto the sample surface has been turned off, the ESR spectra of the $^3P_2$ centres in these cryocrystals disappear despite the fact that the surface of the Ar or Kr cryocrystal, having already condensed, is exposed to the VUV helium gas-discharge irradiation. This means that there is no noticeable contribution to the above-described processes from the He gas-discharge VUV irradiation to which the growing noble-gas cryocrystals are exposed. Nevertheless, the process may be thought of as one in which the He gas-discharge VUV irradiation with photon energies of more than 21 eV performs photoionization of free Ar or Kr atoms close to the surface of the related growing cryocrystal, followed by trapping in the growing cryocrystal of some of the Ar^+ or Kr^+ ions and electrons produced by photoionization. Then, with all the above-discussed processes involved in the cryocrystal, internal ionization would be feasible to proceed. In this case, ESR signals of the $^3P_2$ centres are bound to disappear as the Ar or Kr gas flow is turned off. It is hard to tell whether such a contribution from the photoionized free atoms to the effects observed in the cryocrystals which are described above exists and also whether the contribution of the photoionized atoms is at all comparable with the action of the trapped metastable He atoms.

Acknowledgment

The research described in this publication was made possible in part by grant N R6J000 from the International Science Foundation.

References

Belov A G, Yurtaeva E M and Svishchev V N 1981 *Fiz. Nizk. Temp.* **7** 350–60
Schwentner N, Koch E E and Jortner J 1985 *Electronic Excitations in Condensed Rare Gases* (Berlin: Springer)
Zhitnikov R A and Dmitriev Yu A 1993 *Low. Temp. Phys.* **19** 437–41
—— 1994 *J. Phys.: Condens. Matter* **6** 2727–38
Zhitnikov R A, Dmitriev Yu A and Kaimakov M E 1991 *Sov. Phys.–JETP* **72** 1009–15
—— 1992 *Sov. J. Low Temp. Phys.* **18** 532–8